Mon. Not. R. Astron. Soc. 382, 652–656 (2007) doi:10.1111/j.1365-2966.2007.12390.x

# The baryonic and dark matter properties of high-redshift gravitationally lensed disc galaxies

P. Salucci,[1]* A. M. Swinbank,[2] A. Lapi,[1] I. Yegorova,[1] R. G. Bower,[2] Ian Smail[2] and G. P. Smith[3]

[1]*Astrophysics Sector, SISSA/ISAS, Via Beirut 2-4, I-34014 Trieste, Italy*
[2]*ICC, Department of Physics, Durham University, South Road, Durham DH1 3LE*
[3]*School of Physics and Astronomy, University of Birmingham, Edgbaston, Birmingham B15 2TT*

Accepted 2007 August 29. Received 2007 August 6; in original form 2007 March 22

**ABSTRACT**

We present a detailed study of the structural properties of four gravitationally lensed disc galaxies at $z = 1$. Modelling the rotation curves on sub-kpc scales, we derive the values for the disc mass, the reference dark matter density and core radius, and the angular momentum per unit mass. The derived models suggest that the rotation curve profile and amplitude are best fitted with a dark matter component similar to those of local spiral galaxies. The stellar component also has a similar length-scale, but with substantially smaller masses than similarly luminous disc galaxies in the local Universe. Comparing the average dark matter density inside the optical radius, we find that the disc galaxies at $z = 1$ have larger densities (by up to a factor of $\sim$7) than similar disc galaxies in the local Universe. Furthermore, the angular momentum per unit mass versus reference velocity is well matched to the local relation, suggesting that the angular momentum of the disc remains constant between high redshifts and the present day. Though statistically limited, these observations point towards a spirals' formation scenario in which stellar discs are slowly grown by the accretion of angular momentum conserving material.

**Key words:** gravitational lensing – dark matter – galaxies: spiral.

## 1 INTRODUCTION

It has long been known that the kinematics of spiral galaxies do not show Keplerian fall-off in their rotation curves (RCs), but rather imply the presence of an invisible mass component in addition to the stellar and gaseous discs (Rubin, Thonnard & Ford 1980; Bosma 1981; Persic & Salucci 1988). In the local Universe, by observing the distribution of star light and mapping the gaseous component through H I it has been possible to build up a picture of the how the baryonic component of disc galaxies is distributed and how this relates to the underlying dark matter (DM) component (e.g. Persic, Salucci & Stel 1996). Tracing the evolution of galaxy mass from high redshifts up to the present day is only truly reliable if we can observe the same components at early times. A pioneering study was performed by Vogt et al. (1996) where a handful of RCs of objects at $z \sim 0.5$ were obtained using traditional long-slit spectroscopy on the 10-m Keck Telescope. However, at higher redshifts (e.g. $z \gtrsim 1$) galaxies are much fainter and have smaller angular disc scalelengths than galaxies observed at low redshifts; therefore, obtaining the spatial information required for detailed studies is beyond the limits of current technology. Indeed, mapping the internal properties and dynamics of both the stellar and gaseous components of galaxies at high redshifts is one of the main science drivers for the next generation of ground-based and space-borne telescopes at many wavelengths (e.g. ELT, NGST, ALMA).

One way to overcome this problem is to use the natural amplification caused by gravitational lensing to boost the size and flux of distant galaxies which serendipitously lie behind massive galaxy clusters. This technique is extremely useful since we are able to target galaxies which would otherwise be too small and faint to ensure a sufficiently high signal-to-noise ratio spectroscopy in conventional observations. As such, gravitational lensing has been extensively used to make detailed studies of distant galaxies: for a galaxy at $z = 1$ with an amplification factor of 10, an angular scale of 0.6 arcsec can correspond to $\lesssim$0.5 kpc, sufficient to map also a small spiral.

The benefits of gravitational lensing are complemented by Integral Field Spectroscopy (which produces a contiguous *two-dimensional velocity* map at each point in the target galaxy). This allows a clean decoupling of the spatial and spectral information, thus eliminating the problems arising from their mixing in traditional long-slit observations. It is therefore much easier to identify and study galaxies with regular (bisymmetric) velocity fields.

*E-mail: salucci@sissa.it

In this paper, we present a detailed study of four RCs extracted from disc galaxies which have been observed through the cores of massive galaxy cluster lenses. These targets are taken from the recent work of Swinbank et al. (2003, 2006). They were observed with the Gemini-North Multi-Object Spectrograph Integral Field Unit (GMOS IFU).[1] We concentrate on the galaxy dynamics as traced by the [O II]$\lambda\lambda$3726.1,3728.8 Å emission-line doublet. The IFU data provide a map of the galaxy's velocity field in sky coordinates. To interpret this field, the magnification and distortion caused by the gravitational lensing effect are removed using detailed models of the cluster lenses (see Smith et al. 2005; Kneib et al. 1996; Smith 2002, for details). The primary constraints on the lens models are the positions and redshifts of spectroscopically confirmed gravitational arcs in each cluster. The source plane velocity fields of four systems which display regular (bisymmetric) rotational velocity fields that is resembling rotating discs, were reduced to one-dimensional RCs from which the asymptotic terminal velocity was extracted and compared with the galaxy luminosity (Swinbank et al. 2003, 2006). The key advantage of using gravitational lensing to boost the images of distant galaxies is that we are less biased towards the most-luminous galaxies. Whilst observational information on the distribution of the H I discs in galaxies at these early times would be welcome, such observations will have to wait for future instrumentation (e.g. ALMA).

In this paper, we use nebular emission lines to probe the kinematics of the galaxies. We extract one-dimensional RCs from the velocity fields to infer the distribution of stellar and DM components. Finally, we compare our results with similarly luminous disc galaxies in the local Universe. Throughout this paper, we use a cosmology with $H_0 = 72\,\mathrm{km\,s^{-1}}$, $\Omega_0 = 0.3$ and $\Lambda_0 = 0.7$, $t_0 = 13.7$ Gyr.

## 2 DATA

### 2.1 Sample selection

Our sample comes from observations of six gravitational arcs in Swinbank et al. (2006). In order to avoid possible biases, the targets were selected only to be representatives of galaxies in the distant Universe and no attempt was made to select galaxies with relaxed late-type morphology. We did, however, require that arcs were resolved in both spatial dimensions so that a two-dimensional velocity field could be extracted from the IFU data. This restricted our selection to galaxies with moderate magnification. From the sample of six galaxies, four galaxies appear to have (relaxed) bisymmetric velocity fields with late-type morphologies and colours. The RCs from these four galaxies appear regular and we therefore restrict our analysis to these arcs. We stress that the morphology, colours and velocity fields of the four galaxies in this sample all strongly suggest that these galaxies are consistent with late-type spirals (see Swinbank et al. 2006).

### 2.2 Photometry

From our optical/near-infrared imaging, we constrain the spectral energy distribution (SED) of each galaxy. Since the arcs usually lie with a few arcseconds of nearby bright cluster galaxies, we calculate the magnitude of the arcs in various passbands by masking the arc and interpolating the light from the nearby cluster members. The background light is then removed and surface photometry in different bands is obtained.

Using the cluster mass models, the arcs are reconstructed to the source-plane and the geometry and disc-scale parameters of the discs are measured. This is achieved by fitting ellipses to an isophote of the galaxy image using a modified version of the IDL GAUSS2DFIT routine which fits an exponential profile to the two-dimensional light distribution. From this, the ellipticity, the inclination and luminosities and the disc scalelengths are obtained (see tables 2 and 3 in Swinbank et al. 2006). The latter are also reported below in Table 1.

**Table 1.** Derived structural parameters from the RC mass modelling. Error bars for $M_D$ are shown in Fig. 2, while the uncertainties in $r_0$, $v_{0h}$, $R_{opt} \equiv 3.2\,R_D$ and $\rho_0$ amount to 30, 15, 15 and 40 per cent, respectively.

| Arc | $z$ | $M_D$ ($10^{10}\,M_\odot$) | $r_0$ (kpc) | $\rho_0$ ($10^{-23}\,\mathrm{g\,cm^{-3}}$) | $R_{opt}$ (kpc) | $v_{rot}$ ($\mathrm{km\,s^{-1}}$) |
|---|---|---|---|---|---|---|
| | | | Properties of the galaxies | | | |
| A2390 | 0.912 | 0.40 | 3.1 | 1.4 | 8.3 | 151 |
| RGB1745 | 1.056 | 0.18 | 4.2 | 0.37 | 9.6 | 104 |
| A2218 | 1.034 | 1.70 | 5.8 | 0.64 | 7.7 | 166 |
| Cl2236 | 1.116 | 0.12 | 1.4 | 3.2 | 5.4 | 101 |

### 2.3 One-dimensional RCs

In Fig. 1, we show the one-dimensional RCs of the galaxies in our sample. These are extracted by sampling the velocity field along the major-axis cross-section. The zero-point in the velocity is defined using the centre of the galaxy in the reconstructed source-plane image. The error bars for the velocities are derived from the formal $3\sigma$ uncertainty in the velocity arising from Gaussian profile fits to the [O II] emission in each averaged pixel of the data cube. For the mass-modelling analysis, we folded the RCs on the kinematical centre to ensure that any small-scale kinematical substructure is removed.

## 3 MODELLING AND RESULTS

The RCs of local spiral galaxies imply the presence of an invisible mass component, in addition to the stellar and gaseous discs. The paradigm is that the circular velocity field can be characterized by

$$V^2 = V_D^2 + V_H^2 + V_{DH}^2, \tag{1}$$

where the subscripts denote the stellar disc, dark halo and gaseous disc, respectively. From the photometry, we model the stellar component with a Freeman surface density (Freeman 1970):

$$\Sigma_D(R) = \frac{M_D}{2\pi R_D^2}\,e^{-R/R_D}, \tag{2}$$

where $R_D$ is the disc length-scale, while $R_{opt} \equiv 3.2\,R_D$ can be taken as the 'size' of the stellar disc, whose contribution to the circular velocity is

$$V_D^2(x) = \frac{1}{2}\frac{GM_D}{R_D}(3.2x)^2(I_0K_0 - I_1K_1), \tag{3}$$

where $x = R/R_{opt} \equiv R/(3.2R_D)$ and $I_n$ and $K_n$ are the modified Bessel functions computed at $1.6x$. In small spirals, the H I disc is

[1] Programme ID: GN-2003A-Q-3. The GMOS observations are based on observations obtained at the Gemini Observatory, which is operated by the Association of Universities for Research in Astronomy, Inc., under a cooperative agreement with the National Science Foundation (NSF) on behalf of the Gemini partnership: NSF (United States), the Particle Physics and Astronomy Research Council (United Kingdom), the National Research Council (Canada), CONICYT (Chile), the Australian Research Council (Australia), CNPq (Brazil) and CONICET (Argentina).

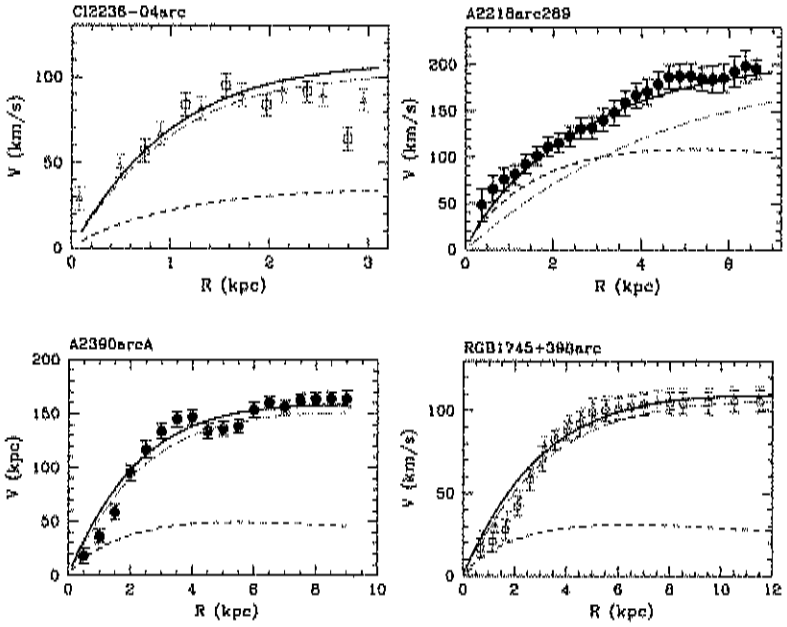


**Figure 1.** The filled circles represent the IFU RCs having enough data to allow the co-addition of the kinematics of the receding and the approaching arms; the red and blue open circles represent the RCs along each arm in the other cases. The DM and stellar components are shown with the long-dashed and short-dashed lines, whilst the model circular velocity is shown with the solid line.

an important baryonic component only for $R > 3R_D$, that is, outside the region considered here. It is plausible that in similar objects also at high redshifts, *inside* $3R_D$, the H I gas contributes to the gravitating baryonic mass by a very small amount, residing at larger radii and it slowly infalls forming the stellar disc.

For the DM component, we take a spherical halo for which $V_H^2(R) = GM_H(< R)/R$. Following the observational scenario constructed in the local Universe (Persic & Salucci 1988; Salucci & Burkert 2000), we assume that it has the Burkert (1995) density profile (see also Salucci et al 2007):

$$\rho(R) = \frac{\rho_0 r_0^3}{(R + r_0)\left(R^2 + r_0^2\right)}, \tag{4}$$

where $r_0$ is the core radius and $\rho_0$ is the effective core density. It follows that

$$M_H(R) = k\left[\ln\left(1 + \frac{R}{r_0}\right) - \tan^{-1}\left(\frac{R}{r_0}\right) + \frac{1}{2}\ln\left(1 + \frac{R^2}{r_0^2}\right)\right] \tag{5}$$

with $k = 6.4\,\rho_0 r_0^3$ and of course $V_H^2(R) = GM_H(R)/R$. We note that the adopted velocity profile is a quite general: it allows a distribution with a core of size $r_0$, converges to the Navarro–Frenk–White (NFW) profile at large distances and, for suitable values of $r_0$, can also mimic the NFW or an isothermal profile, over the limited region of galaxy which is mapped by the RCs.

The mass model has three free parameters: the disc mass $M_D$, the core radius $r_0$, and the central core density $\rho_0$. The observations extend out to approximately $(2–3)R_D$, have 10–60 independent measurements with an observational error of 3–10 per cent in their amplitude, and of 0.05–0.2 in their slopes $\mathrm{d}\log V/\mathrm{d}\log R$. The error in the estimate of the disc inclination angles is negligible with respect to the above. These errors are (understandably) higher than those associated with the best-quality local RCs and make it difficult to constrain the halo density profile $\rho(R)$. However, they are sufficiently small to yield a reliable value for the halo mass, the average density inside a reference radius [which we chose to be $R_2 = 2\,R_D$ so that $\langle\rho\rangle = M_H(R_2)/(4/3\,\pi\,R_2^3)$] and the disc mass and a reasonable estimate of the 'core radius'.

By reproducing the observed RCs with the models given by equations (1)–(5), we derive the best-fitting parameters for each galaxy and overlay the resulting mass model on to each RC in Fig. 1. In Table 1, we report the main structural parameters: the disc mass, the halo core radius, $\rho_0$, the optical radius $R_{opt}$ and $v_{0h} = V_H(R_{opt})$, that is, the halo contribution to circular velocity at the optical radius.

In all our RCs, the *amplitude* and the *profile* of the stellar disc contribution cannot reproduce the observed RC rise between $1.5R_D$ and the last measured radius. This strongly suggests evidence for the presence, at $z \approx 1$, of a DM component of mass comparable to that found for local disc galaxies with similar $V_{opt}$ (see figs 2, 8 and 9 of Persic et al. 1996). We derive disc masses ranging between $1 \times 10^9$ and $2 \times 10^{10}\,M_\odot$ for galaxies with the reference velocity $V_{opt}$ between 100 and 200 km s$^{-1}$. These disc masses are smaller by a factor of 2–4 than those of the local spirals with the same reference velocity which are shown to follow Inner Baryon Dominance (see Salucci & Persic 1999). The high-redshift stellar discs are submaximal discs. Forcing a maximal disc even in the 'weak' implementation of Persic & Salucci (1990) leads to unacceptable fits of our high-$z$ RCs.

The best-fitting values for $r_0$ are of the order of $\sim 1.5R_D$, which is larger than usually compatible with an NFW profile, although the error bars on our data preclude any strong statement.

Since the gravitational lens model affects the source-plane reconstruction of the galaxies, we must test for the effect that this has on the resulting RCs. We reconstruct the galaxies using the family of lens models that inhabit the $\Delta\chi^2$ contour corresponding to $1\sigma$ confidence interval relevant to each cluster. For example, the model of RGB 1745 has five free parameters, and the lens modelling uncertainties are therefore derived by considering models within the $\Delta\chi^2 = 5.89$ contour. From each reconstruction, we extract the

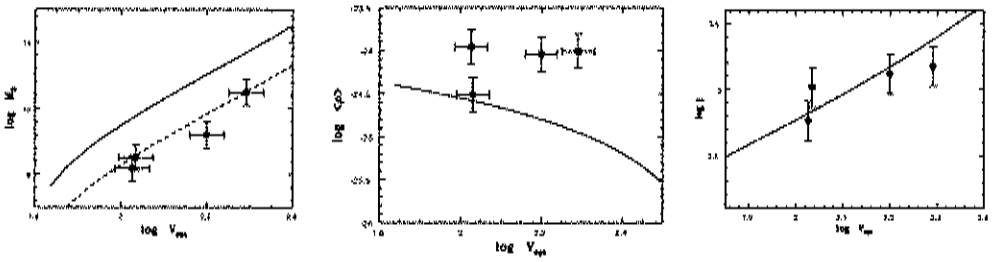

**Figure 2.** Left-hand panel: disc mass (in solar units) versus reference velocity (in km s$^{-1}$) compared with the $z = 0$ relation (solid line) and with this scaled down by 0.6 dex (dashed line). Middle panel: average DM density (in g cm$^{-3}$) versus reference velocity compared with the $z = 0$ relation (solid line). Right-hand panel: disc angular momentum per unit mass $j$ (in km s$^{-1}$ kpc units) versus disc mass compared with the $z = 0$ relation (solid line). The uncertainties on the local relations are: 0.15 dex in $j$, 0.2 dex in $\log M_{\rm D}$ and 0.3 dex in $\log\langle\rho\rangle$.

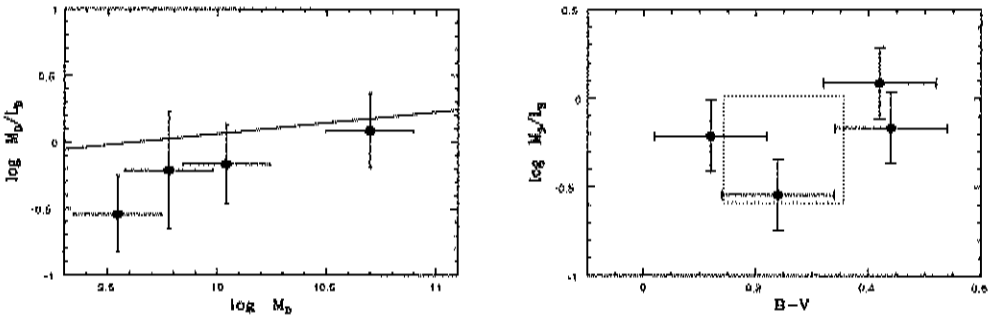

**Figure 3.** Left-hand panel: mass-to-light ratio versus disc mass for the galaxies in our sample compared with the local disc galaxies from Shankar et al. (2006) (solid line). The average offset corresponds to an excess in luminosity by a factor of 4. Right-hand panel: mass-to-light ratio versus colour relations for our sample. The square box denotes the predicted colours from a Bruzual & Charlot single stellar population (see the text for details).

one-dimensional RC and apply the analysis outlined above and find that the maximum variations are: $\Delta\log M_{\rm D} = 0.03$, $\Delta\log\langle\rho\rangle = 0.02$, $\Delta\log(V_{\rm opt}) \lesssim 5\,{\rm km\,s^{-1}}$. Thus, the uncertainties in the gravitational lens modelling are negligible compared to the uncertainties in the RC mass modelling.

A cosmological significance of our result is evident in Fig. 2 where we compare the disc mass, the mean DM density within the optical radius and the angular momentum per unit mass, all as a function of the reference velocity. These are compared to similar properties of the local objects (Shankar et al. 2006). Fig. 2 strikingly shows that high-redshift spirals, modulo an offset of $0.6^{+0.1}_{-0.15}$ dex, are on the same $\log M_{\rm D}$ versus $\log V_{\rm opt}$ relationship found for local spirals arising from the systematic structural properties of their mass distribution (Tonini et al. 2006), see also (Salucci, Frenk & Persic 1993).

In Fig. 2, from the values of $\langle\rho\rangle$, a quantity that differently from $\rho_0$ is weakly affected by the RC $1\sigma$ fitting uncertainties, it is apparent that the DM haloes of $z = 1$ disc galaxies are denser by $0.7^{+0.1}_{-0.2}$ dex than those around similarly luminous $z = 0$ spirals. The evidence that spiral discs at $z = 0$ and 1 have the same structural relationships is further supported by observations of the evolution of the Tully–Fisher (TF) relation (which correlates the disc mass with $V_{\rm opt}$). In our and in other independent samples (Vogt et al. 1996; Bamford et al. 2005; Swinbank et al. 2006), the galaxies at $z = 1$ show a TF relation with a slope similar to that of the local TF relation, but with an offset compatible with that found in this work from the disc mass versus rotation velocity relationship. This suggests that from $z = 1$ to 0, the stellar disc mass $M_{\rm D}$ of a spiral has grown by a factor of $\sim 4^{+1}_{-2}$, that leads to just a modest increase in the DM-dominated quantity $V_{\rm opt}$.

Further evidence that $z = 1$ disc galaxies are related to present-day spirals is provided by the relationship between angular momentum per unit mass ($j$) versus the reference velocity, as shown in Fig. 2. This well theoretically motivated relation (e.g. Tonini et al. 2006) can be considered as the imprint of the process of the formation of discs inside DM haloes related to the cosmological properties of halo spin parameters. As Fig. 2 shows, there appears to be no evolution in this crucial relationship between the the cosmological time at which we observe these spirals, $z = 1, t = 6$ Gyr and the present time, $z = 0, t = 13.7$ Gyr. This agreement is remarkable: it establishes a link between local and high-redshift discs, supporting the idea that the angular momentum remains constant during the evolution of a disc system from high redshifts to the present day.

The kinematical estimate of the disc mass allows us to derive the mass-to-light ratios for our disc systems as a function of luminosity and colour. In Fig. 3, we compare the disc mass and colour as a function of the mass-to-light ratio compared to the relation in local spirals (Shankar et al. 2006). In order to compare directly with local relations, we consider a simple passive evolution model for the luminosity evolution. For a single stellar population, the zero-point of the local relation is decreased by a factor of $\log(13.7/6)$ which accounts for the passive evolution of a *single* stellar population from $z = 1$ to 0. As Fig. 3 shows, the mass-to-light ratios as a function of the galaxy ($B - V$) colour are in broad agreement with predictions of a single stellar population which is $\sim$1 Gyr old (Bruzual & Charlot 2003), although clearly photometry at other wavelengths (such as rest-frame $K$ band) would allow a more detailed decomposition of the stellar populations in these galaxies.

### 3.1 Cosmological implications

Fig. 2 shows that at a radius corresponding to $V_{\rm opt}$ the high-redshift galaxies are significantly denser than comparably luminous local

disc galaxies: the average offset is about 0.6 dex in $\log(\langle\rho\rangle)$. Although we cannot exclude the fact that dynamical processes occur between $z = 1$ and 0 to reduce the DM density in the luminous regions, this offset is naturally explained if the haloes embedding these disc galaxies formed at earlier times than the haloes around similarly massive $z = 0$ spirals. In this framework, we estimate the ratio between the virialization redshift of the local galaxies and and that of the galaxies in our sample. Since $\rho_v \propto \Delta(z_v)(1+z_v)^3$, where $\rho_v$ and $z_v$ are the average density and redshift at virialization and $\Delta_v$ is known, for $z_0 = 1$, $z_v = 1.7$, which corresponds to $t_v = 6$ Gyr.

Assuming that our sample is a fair representation of disc galaxies at $z \sim 1$ and that these are approximately coeval, from the comparison of their structural properties with those of $z = 0$ spirals, the following simple picture emerges: a present-day spiral, with a given circular velocity, half-light radius and the angular momentum per unit mass, at redshift 1 had similar values for these quantities, but a smaller stellar mass: $\langle M_\star(t_{\rm obs})/M_\star(t_0)\rangle \simeq 0.3$. This induces a scale for the average star formation rate (SFR) in the past 8 Gyr: $\sim 0.75 M_\star(t_0)/(t_{\rm obs} - t_0) \sim 1\ M_\star(t_0)/(10^{10}\,{\rm M}_\odot)\,{\rm M}_\odot\,{\rm yr}^{-1}$. With these discs having an average age of 1 Gyr at $z = 1$, we can also derive an 'early-times' average SFR $\sim 0.25\ M_\star(t_0)/(1\,{\rm Gyr}) \sim 3\ M_\star(t_0)/(10^{10}\,{\rm M}_\odot)\,{\rm M}_\odot\,{\rm yr}^{-1}$ which points towards a declining SFR history.

The marked increase in the luminosity per unit stellar mass in objects at high redshifts with respect to their local counterparts has the simplest explanation in a passive evolution of the star-forming discs. Obviously, this simple picture requires us to assume that the high-redshift systems are the direct counterparts of similar rotation speed spirals at low redshifts.

## 4 DISCUSSION AND CONCLUSIONS

In this study, we have investigated the detailed properties of four disc galaxies at $z = 1$. These galaxies were observed at a high spatial resolution, thanks to the boost in angular size provided by gravitational lensing by foreground massive galaxy clusters and allow a much more detailed comparison with local populations than usually possible for galaxies at these early times. Modelling the one-dimensional RCs with those of Persic et al. (1996), we derive best-fitting parameters for the total dynamical mass, the core radius, the effective core density and the angular momentum per unit mass.

The best-fitting model RCs to the data show that the amplitude and profile of the stellar disc components cannot unambiguously reproduce the rise in the RC without a DM component. Comparing the average DM density inside the optical radius, we find that the disc galaxies at $z = 1$ have larger densities (by up to a factor of $\sim$7) than similar disc galaxies in the local Universe. In comparison, we find that the angular momentum per unit mass versus reference velocity is well matched to the local relation suggesting that the angular momentum of the disc remains constant between high redshifts and the present day. Though statistically limited, these observations point towards a spirals' formation scenario in which stellar discs are slowly grown by the accretion of angular momentum conserving material. Our result is also consistent with the theoretical evolution of the angular momentum of discs from semi-analytic models from $z = 1$ to 0 which show the modest offset of $\Delta j \lesssim 0.2\,{\rm kpc\,km\,s^{-1}}$ for objects with circular velocities between 50 and 300 $\rm km\,s^{-1}$ (Cole et al. 2000; Bower et al. 2006). These results provide an evolutionary link between the disc systems we observe at a redshift $z \sim 1$ and the present-day population of spirals.

While these results are based on data of only four objects, they nevertheless show the power which gravitational lensing can have on studying the internal properties of high-redshift galaxies. In particular, these observations should be viewed as pathfinder science which will soon be routine with Adaptive Optics Integral Field Unit observations on 8- and 10-m telescopes (e.g. Genzel et al. 2006). Moreover, by combining these results with upcoming telescopes and instruments (e.g. ALMA) which will be sensitive enough to map the H I content of galaxies to $z = 1$, the exact relation between gas, stars and DM can be probed in much more detail.

## ACKNOWLEDGMENTS

We would like to thank the anonymous referee for his/her suggestions which improved the content and clarity of this paper. We thank Carlton Baugh for providing the theoretical evolution of disc mass in galaxies from GALFORM. We also thank Gigi Danese for useful discussions. AMS acknowledges support from a PPARC Fellowship, RGB acknowledges a PPARC Senior Fellowship and IS and GPS acknowledge support from the Royal Society.

## REFERENCES

Bamford S. P., Milvang-Jensen B., Aragón-Salamanca A., Simard L., 2005, MNRAS, 361, 109
Bosma A., 1981, AJ, 86, 1825
Bower R. G., Benson A. J., Malbon R., Helly J. C., Frenk C. S., Baugh C. M., Cole S., Lacey C. G., 2006, MNRAS, 370, 645
Bruzual G., Charlot S., 2003, MNRAS, 344, 1000
Burkert A., 1995, ApJ, 447, L25
Cole S., Lacey C. G., Baugh C. M., Frenk C. S., 2000, MNRAS, 319, 168
Freeman K. C., 1970, ApJ, 160, 811
Genzel R. et al., 2006, Nat, 442, 786
Kneib J.-P., Ellis R. S., Smail I., Couch W. J., Sharples R. M., 1996, ApJ, 471, 643
Persic M., Salucci P., 1988, MNRAS, 234, 131
Persic M., Salucci P., 1990, MNRAS, 247, 349
Persic M., Salucci P., Stel F., 1996, MNRAS, 281, 27
Rubin V. C., Thonnard N., Ford W. K., Jr, 1980, ApJ, 238, 471
Salucci P., Burkert A., 2000, ApJ, 537, L9
Salucci P., Persic M., 1999, A&AP, 351, 442
Salucci P., Frenk C. S., Persic M., 1993, MNRAS, 262, 392
Shankar F., Lapi A., Salucci P., De Zotti G., Danese L., 2006, ApJ, 643, 14
Smith G. P., 2002, PhD thesis, University of Durham
Smith G. P., Kneib J.-P., Smail I., Mazzotta P., Ebeling H., Czoske O., 2005, MNRAS, 359, 417
Swinbank A. M. et al., 2003, ApJ, 598, 162
Swinbank A. M., Bower R. G., Smith G. P., Smail I., Kneib J.-P., Ellis R. S., Stark D. P., Bunker A. J., 2006, MNRAS, 368, 1631
Tonini C., Lapi A., Shankar F., Salucci P., 2006, ApJ, 638, L13
Vogt N. P., Forbes D. A., Phillips A. C., Gronwall C., Faber S. M., Illingworth G. D., Koo D. C., 1996, ApJ, 465, L15

This paper has been typeset from a TEX/LATEX file prepared by the author.